Post Hatfield rolling contact fatigue

The effect of residual stress on contact stress driven crack growth in rail

Part 2: Data

A Kapoor and DI Fletcher

November 2006
NewRail Report No. WR061106-3

NewRail | School of Mechanical & Systems Engineering | Newcastle University
NE1 7RU | UK | T+44 (0)191 222 5821 |F+44 (0)191 222 5821 | www.newrail.org

OFFICE OF RAIL REGULATION

The majority of the work reported here was undertaken at the University of Sheffield in 2003-2004, but publication was embargoed until 2006. The authors are now at Newcastle University. This issue supersedes earlier versions of the report.

Contents

1 Summary **3**

2 Branching criterion **4**

3 Runs undertaken **5**

4 Results and discussion **5**
4.1 The effect of residual stress on crack growth angle 5
4.2 Sensitivity of crack growth rate to the magnitude of residual stress 9
4.3 Sensitivity of crack growth rate to continuously welded rail stress 10
4.4 Effect of crack angle on crack growth rate 12
4.5 Effect of contact parameters on crack growth rates 14
4.5.1 Contact pressure 14
4.5.2 Crack face friction 14
4.5.3 Surface and crack face friction 16

5 Conclusions **17**

1 Summary

Runs of the model developed and described in the previous report [1] were undertaken to investigate the effect of residual stress and continuously welded rail (CWR) stress on crack growth in rails. The areas investigated were:

- Prediction of crack growth rates and directions, and how residual stress affects these
- The effect of CWR stress on crack growth rate, including when it acts in combination with residual stress
- The way in which initial crack angle affects the influence residual stresses have on crack propagation rates
- The effect of contact pressure, surface friction and crack face friction on the crack growth rate in the presence of residual stress

It was found that:

- The inclusion of residual stress in the modelling of a crack at 30° below the rail surface produced a tendency for the crack to branch down into the rail, but this effect does not begin until the crack exceeds 20-25mm in length.
- Tensile CWR stress (cold rails) could produce around a 70% rise in crack growth rate over that of no CWR stress. Compressive residual stresses (hot rails) had almost no effect on crack growth rates.
- Without residual stresses crack growth rate was predicted to increase with increasing crack angle. With residual stresses present this trend was reversed, with 30° cracks showing the highest growth rates, and the growth rate of cracks of 60° or above showing insensitivity to crack angle.
- Trends in crack growth rate with variations in contact pressure, crack face friction and surface friction levels were largely similar for cases with and without residual stresses applied.

This report contains revised information on the residual stress input data, and supersedes earlier versions of the report.

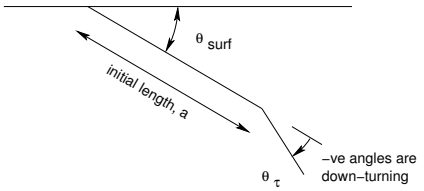

Figure 1: Definition of crack growth and branching angles

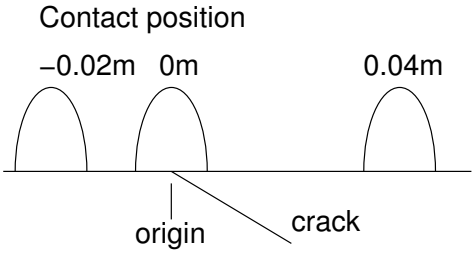

Figure 2: Schematic illustration of contact position.

2 Branching criterion

The branching criterion used was described in full in the project literature review [2]. Briefly, the method used was that developed by Kaneta et al. [3] based on the maximum shear stress theories (Equations 1) adapted for non-proportional loading present in rolling contact fatigue situations. The definition of the original crack angle and the branch angle are given in Figure 1. Kaneta et al. showed that the direction of branch crack growth (θ_τ) can be found by taking the root of Equation (2) relative to the initial crack growth direction which gives the maximum value of the equivalent shear mode stress intensity factor K_τ . Crack growth angle and branching angles are defined by Figure 1

$$K_\tau = \frac{1}{2}\cos\frac{\theta_\tau}{2}\left[K_I \sin\theta_\tau + K_{II}(3\cos\theta_\tau - 1)\right] \tag{1}$$

$$\tan^3\frac{\theta_\tau}{2} - \frac{1}{\gamma}\tan^2\frac{\theta_\tau}{2} - \frac{7}{2}\tan\frac{\theta_\tau}{2} + \frac{1}{2\gamma} = 0, \gamma = \frac{K_{II}}{K_I} \tag{2}$$

The values of K_I and K_{II} at instants throughout the stress cycle (i.e. at each contact position, see Figure 2) are used to calculate crack growth direction from Equation (2) evaluated at each instant, producing a range of resultant K_τ and θ_τ values. The question of which of these resultant values actually governs crack growth direction is not really resolved by the method, but it is assumed that the crack will propagate in the direction corresponding to the maximum resultant or K_τ. For models including the crack face friction Kaneta et al. [3] found that in the absence of fluid pressure and crack face friction growth is always by shear, and takes place close to the line of the original crack. The actual angle is given as θ_τ, the solution to equation (1).

3 Runs undertaken

The 2.5d (elliptical contact) crack growth model [1] was used for all the runs detailed in this report. The runs are summarised in Table 1. Measured residual stresses specific to the Hatfield rail were not available so it was decided to use values from the literature [2] in the investigation. These values were also used in the work reported previously [1], and are used in all runs including residual stress unless stated otherwise. Runs were completed with both the standard residual shear stress values (marked + in the table), and with values reversed (multiplied by -1, marked - in the table).

Contact pressure was related to contact size using Equation (3) [4]. Here area is in mm^2 and contact pressure in MPa.

$$area = 11923 P_0^{-0.6818} = \pi ab = \pi E a^2 \tag{3}$$

The crack growth law used to convert between stress intensity factors and crack growth rates is summarised by Equations (4) and (5). Full details can be found in the previous project report [1].

$$\frac{da}{dN} = 0.000507(\Delta K_{eq}^{3.74} - 4^{3.74}) \tag{4}$$

$$\Delta K_{eq} = \sqrt{\Delta K_I^2 + \left[\left(\frac{614}{507}\right)\Delta K_{II}^{3.21}\right]^{\frac{2}{3.74}}} \tag{5}$$

The growth rate da/dN is given in nm per cycle, and the stress intensity factors are in MPa$\sqrt{m}$. Equations (4) and (5) were developed at the University of Sheffield [5].

4 Results and discussion

4.1 The effect of residual stress on crack growth angle

Figure 3 and 4 show the variation of predicted crack growth angle with movement of the contact across the crack (contact position is defined in Figure 2). Also shown in the plots is the equivalent shear mode stress intensity factor which describes the stress driving the crack growth. As discussed above, the predicted growth angle changes with contact position because the ratio of mode I (K_I) and mode II (K_{II}) stress intensity factors changes with contact position. To identify a single angle at which growth can be assumed to occur, Kaneta et al. [3] recommend taking the angle at which the driving stress intensity factor is largest. Because the current work considers crack growth in shear, positive and negative values of stress intensity factor correspond simply to the crack sliding in one direction or the other. Either direction may produce crack growth, so both must be considered.

Looking first at the predictions for the case without residual stress (Figure 3) peaks in stress intensity factor occur at contact positions of approximately 0.05m and 0.03m. The corresponding branching angles are zero and $-3.8°$. These results are for a crack length (i.e crack radius since the cracks are taken to be semi-circular) of 28mm, and are similar to those calculated by Kaneta et al. [3] for similar shear mode crack growth configurations. The peaks in stress

Run no.	P_0 MPa	Residual stress	Shear sign	CWR MPa	Angle deg	μ	μ_{cf}
3	1500	-		-	30	0.18	0.18
15	1500	Standard	+	-	30	0.18	0.18
17	1500	Standard	-	-	30	0.18	0.18
44	1500	+25%	+	-	30	0.18	0.18
46	1500	-25%	+	-	30	0.18	0.18
51	750	Standard	+	-	30	0.18	0.18
54	3000	Standard	+	-	30	0.18	0.18
56	1500	Standard	+	-	30	0.30	0.30
57	1500	Standard	+	-	30	0.05	0.05
58	1500	Standard	+	-	30	0.30	0.18
59	1500	Standard	+	-	30	0.30	0.05
60	1500	-		100	30	0.18	0.18
61	1500	-		-100	30	0.18	0.18
62	1500	Standard	+	100	30	0.18	0.18
63	1500	Standard	+	-100	30	0.18	0.18
64	1500	Standard	-	100	30	0.18	0.18
64	1500	Standard	-	-100	30	0.18	0.18
76	1500	Standard	+	-	35	0.18	0.18
77	1500	Standard	+	-	40	0.18	0.18
78	1500	Standard	+	-	45	0.18	0.18
79	1500	Standard	+	-	60	0.18	0.18
80	1500	Standard	+	-	75	0.18	0.18
81	1500	Standard	+	-	80	0.18	0.18
82	1500	Standard	+	-	85	0.18	0.18
83	1500	Standard	+	-	90	0.18	0.18
84	1500	-		-	35	0.18	0.18
85	1500	-		-	40	0.18	0.18
86	1500	-		-	45	0.18	0.18
87	1500	-		-	60	0.18	0.18
88	1500	-		-	75	0.18	0.18
89	1500	-		-	80	0.18	0.18
90	1500	-		-	85	0.18	0.18
91	1500	-		-	90	0.18	0.18
92	750	-		-	30	0.18	0.18
93	3000	-		-	30	0.18	0.18
94	1500	-		-	30	0.30	0.30
95	1500	-		-	30	0.05	0.05
96	1500	-		-	30	0.30	0.18
97	1500	-		-	30	0.30	0.05

Table 1: Conditions examined. Runs 3 and 15 were detailed in the previous report [1]. All runs were conducted using the 2.5d model. When residual stress was applied, all longitudinal, vertical and shear stresses were included in each run. Runs were completed with both the standard residual shear stress values (marked + in the table), and with values reversed (marked - in the table). Run numbers are not sequential because some runs were not useful, and are not reported.

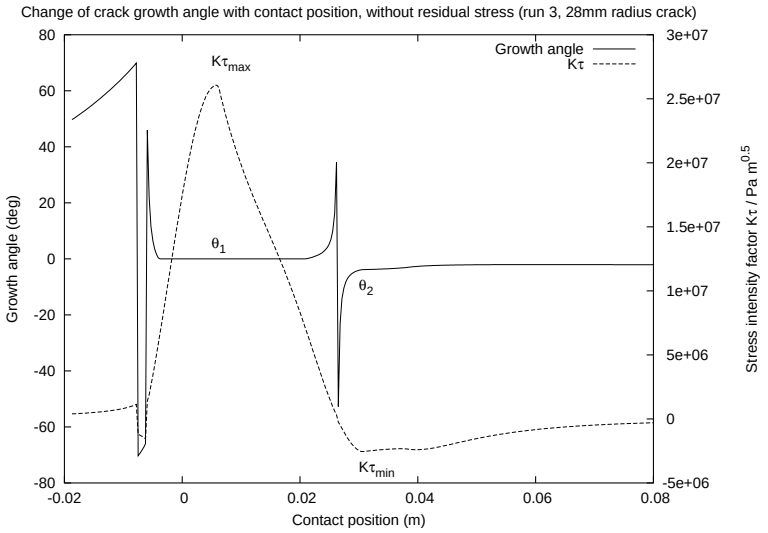

Figure 3: Variation of crack branch angle and equivalent shear mode stress intensity factor with contact position for a 28mm radius crack. No residual stress, maximum Hertzian contact pressure 1500MPa, surface and crack face friction coefficient 0.18 (run 3).

intensity factor are of opposite sign, representing alternate sliding directions for the crack, but the positive peak is around 10 times the magnitude of the negative, so the dominant angle is likely to be zero degrees, i.e the crack is predicted to continue ahead on its existing path at 30° below the rail surface.

With the addition of residual stress the contact positions at which peaks in stress intensity factor occur change slightly (Figure 4) but the predicted angles of branch crack growth change substantially. The higher peak now corresponds to a branch angle of nearly $-9°$ while the lower peak corresponds to an angle of around $-3.2°$. These negative angles represent down-turning crack branching. With the addition of residual stress the stress intensity factors remain negative throughout the passage of the contact over the crack. The true "peak" in stress intensity factor is therefore at $K\tau_{min}$, for which the predicted branch angle is around $-3.2°$.

To bring together results for a variety of crack lengths, Figure 5 shows the predicted crack branch angles for a wide range of crack lengths. Cracks with and without residual stress applied are included, and the angles corresponding to both the upper and lower peaks in stress intensity factor are plotted. It can be seen that without residual stress applied it is predicted that the crack will propagate along its original line, or branch down at $2 - 3°$ below its original line. When residual stresses are applied, there is very similar behaviour up to crack lengths of 20 to 25mm, after which there is a much stronger tendency for the cracks to branch down. It should be emphasised that Figure 5 does not

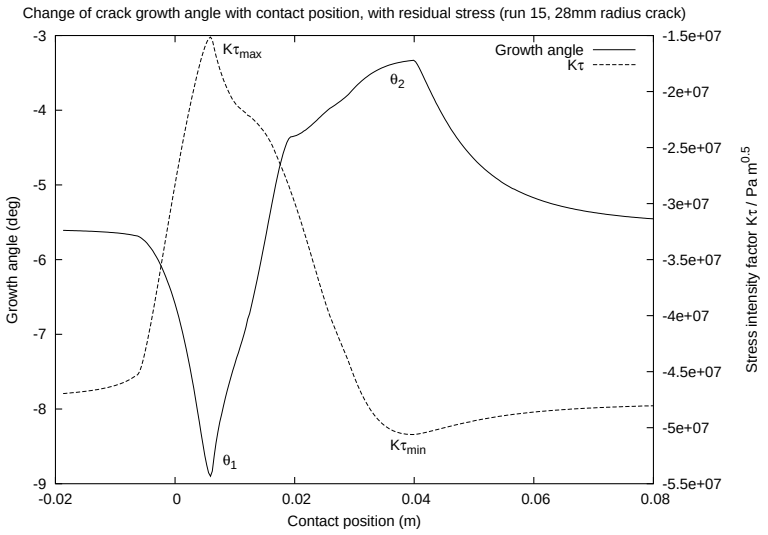

Figure 4: Variation of crack branch angle and equivalent shear mode stress intensity factor with contact position for a 28mm radius crack. Residual stress included, maximum Hertzian contact pressure 1500MPa, surface and crack face friction coefficient 0.18 (run 15).

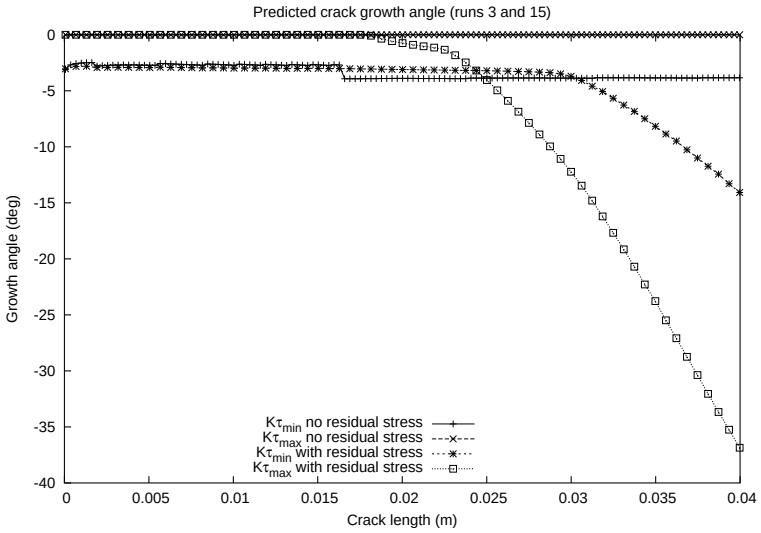

Figure 5: Variation of crack branch angle with crack length. Residual stress included, maximum Hertzian contact pressure 1500MPa, surface and crack face friction coefficient 0.18 (runs 3 and 15). Initial crack at 30° below the rail surface.

plot crack trajectories, but indicates the angles at which an unbranched crack of a particular length would tend to branch. It is specific to the residual stress input data used, and is of for cracks initially at 30° below a contact of 1500MPa under friction conditions characteristic of water lubrication.

4.2 Sensitivity of crack growth rate to the magnitude of residual stress

Only one set of residual stress input data were available, so to investigate the sensitivity of the model to the residual stress data, runs were performed in which the magnitude of these stresses was varied by ±25% of their original value. The results of these runs are plotted in Figure 6

The results indicated that the application of any level of residual stress increased crack growth rate above the case without residual stress for all the crack lengths investigated. At length up to around 25mm (the most important for shallow angle crack growth) the crack growth rate for cases with residual stress applied varied disproportionately with the change in residual stress. Taking the peak crack growth rates in this range of crack lengths, increasing the residual stress by 25% produced almost a 50% increase in growth rate. Decreasing the residual stress by 25% produced only around a 20% drop in crack growth rate. The changes in growth rate were reversed at longer crack lengths, for which the residual stress in the center of the rail head, rather than at the surface, is important. Here an increase in residual stress of 25% decreased crack growth rate by

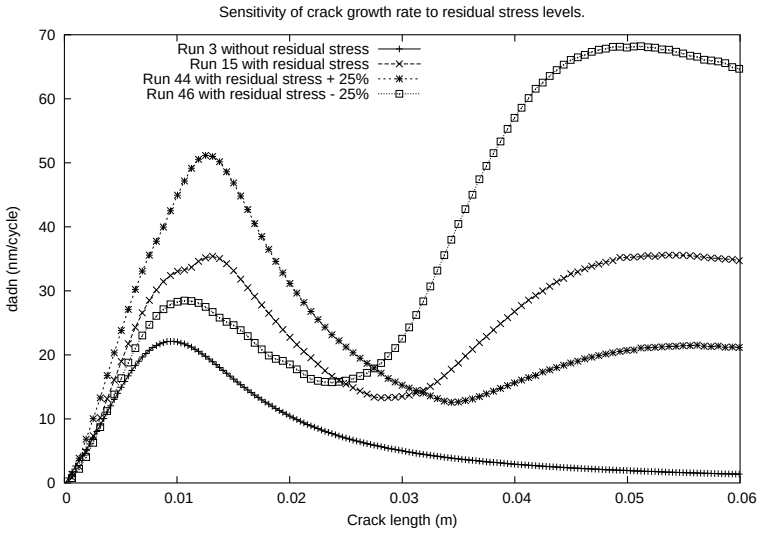

Figure 6: Sensitivity of crack growth rate to the magnitude of residual stress. Residual stress applied, including variation by ±25%, maximum Hertzian contact pressure 1500MPa, surface and crack face friction coefficient 0.18.

around 40%, while decreasing it by 25% gave a crack growth increase of almost 80%. This pattern of changes is almost certainly a function of the distribution of compressive and tensile regions in the residual stress distribution, but this has not been further investigated.

4.3 Sensitivity of crack growth rate to continuously welded rail stress

The effect of temperature on the longitudinal stress in rails was reported in the project literature review [2] where it was found that a change of 1°C produces a change of around 2.5MPa in longitudinal rail tension, or continuously welded rail stress (CWR). Taking an extreme case of rail temperature varying ±40°C either side of the rail neutral temperature (the stress free temperature) gives a longitudinal stress which may vary ±100MPa. Figure 7 shows the effect on crack propagation rates of this change in stress, and also includes the case of contact loading only with zero longitudinal stresses. No residual stresses are included in this case. It is shown that the application of compressive CWR stress (i.e. a rail heated above its neutral temperature) makes almost no difference to the crack growth rate. Application of the tensile CWR stress (i.e rail cooled below its neutral temperature) gives a rise of around 70% in crack growth rate.

The disproportionate effect of positive and negative CWR stress is thought to be due to the effect of this longitudinal stress on crack closure. Under contact loading the crack is closed for much of the passage of the contact (the faces of

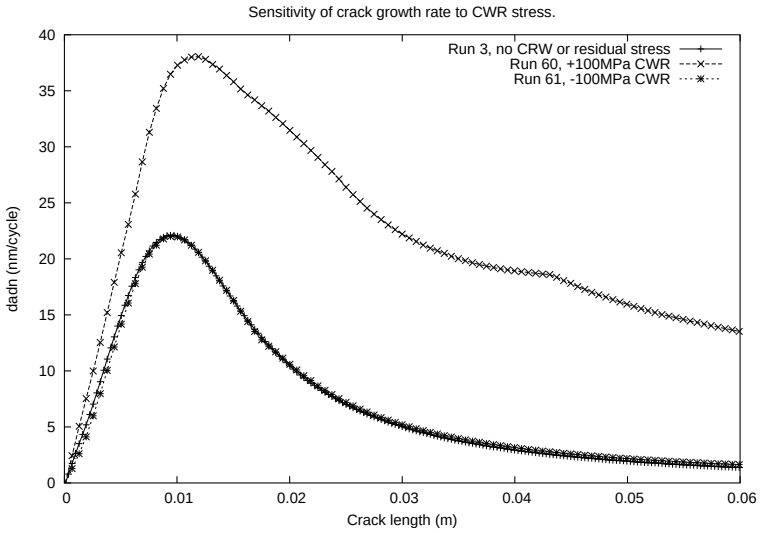

Figure 7: Sensitivity of crack growth rate to continuously welded rail (CWR) stress. CWR stresses of ±100MPa represent approximately ±40°C either side of the rail neutral temperature. Maximum Hertzian contact pressure 1500MPa, surface and crack face friction coefficient 0.18.

an inclined crack are pressed together by the load above it). Application of a compressive CWR stress will apply greater pressure between the crack faces, and may restrict their ability to slide over one another, however, the results show that any effect is small. Application of tension to the rail will open the crack, or at least reduce the stress pressing its faces together. This will allow the faces to move over one another much more freely than when it is pressed tightly shut, allowing a large increase in stress intensity factor, and hence in crack growth rate. Details of the influence of friction between the crack faces (often referred to as crack face friction) on crack growth is given in the previous report [1], and is further investigated in Section 4.5.

Application of CWR stress in addition to residual stress and contact stress was investigated in runs 15, 17 and 62-65, the results of which are plotted in Figures 8 and 9. The sign of the residual shear stress applied is changed between Figures 8 and 9 [1].

The results for combined application of residual and CWR stress show very similar results to the application of CWR stress alone. At short crack lengths the results for the case without CWR stress and with -100MPa CWR stress are almost identical, for both the positive and negative shear stresses. Application of the positive 100MPa CWR stress increases the predicted crack growth rate more in the case of positive shear stress (130% increase in peak crack growth rate) than negative shear stress (80% increase). Both these increases exceed that for CWR stress alone, which shows approximately a 38% increase in peak growth rate. At longer crack lengths the crack growth rates in the presence

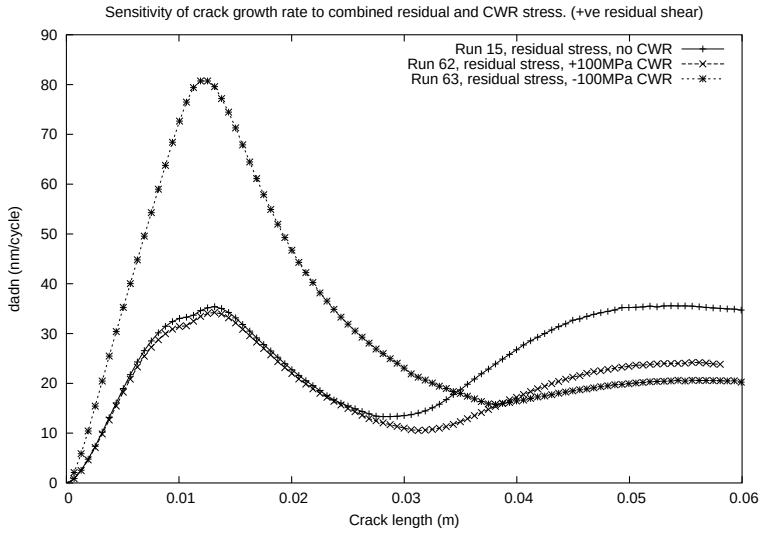

Figure 8: Sensitivity of crack growth rate to continuously welded rail (CWR) stress in the presence of residual stress. Residual stress applied with positive shear stress. CWR stresses of ±100MPa represent approximately ±40°C either side of the rail neutral temperature. Maximum Hertzian contact pressure 1500MPa, surface and crack face friction coefficient 0.18.

of CWR stress were reduced below those for no CWR stress. This occurred regardless of the sign of the CWR stress. As for other cases reported, it should be remembered that these results are specific to the input conditions and crack geometry modelled.

4.4 Effect of crack angle on crack growth rate

The effect of residual stress on crack growth is dependent on the angle of the crack within the rail, because crack angle affects the degree to which vertical and horizontal components of residual stress act on the crack. The runs discussed above, and those in the previous report [1], are for cracks at 30° below the rail surface. Figure 10 shows how crack growth rate is affected by changing the initial crack angle when residual stress is not present, and Figure 11 shows the effect with residual stress present.

Without residual stress present, the crack at 30° below the rail surface has the slowest crack growth of all those examined. Angles below 30° could not be tested because the Green's functions on which the stress intensity factor results rely are not available for very shallow angled cracks. Application of residual stress changes the ranking of crack growth rate with angle variation completely. Figure 11 shows that with residual stress applied the 30° crack is now predicted to be the fastest growing of all those examined, with the exception of cracks around 30mm long, where the growth rate for 35° cracks is marginally higher.

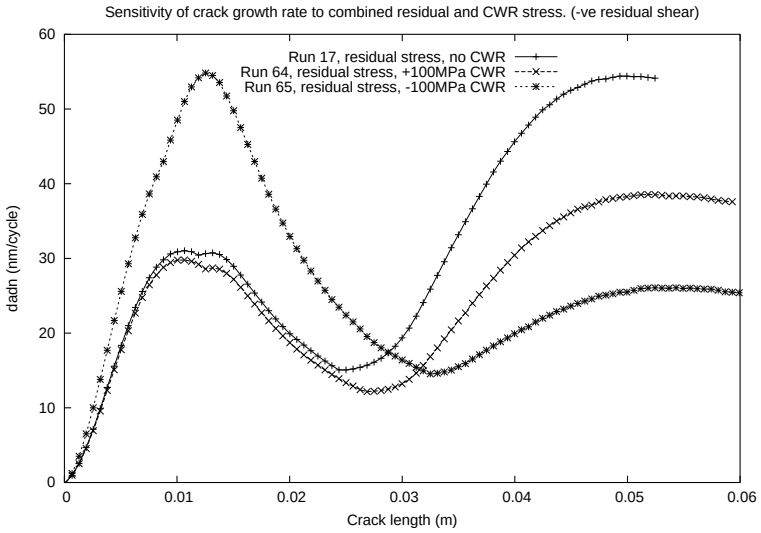

Figure 9: Sensitivity of crack growth rate to continuously welded rail (CWR) stress in the presence of residual stress. Residual stress applied with negative shear stress. CWR stresses of ±100MPa represent approximately ±40°C either side of the rail neutral temperature. Maximum Hertzian contact pressure 1500MPa, surface and crack face friction coefficient 0.18.

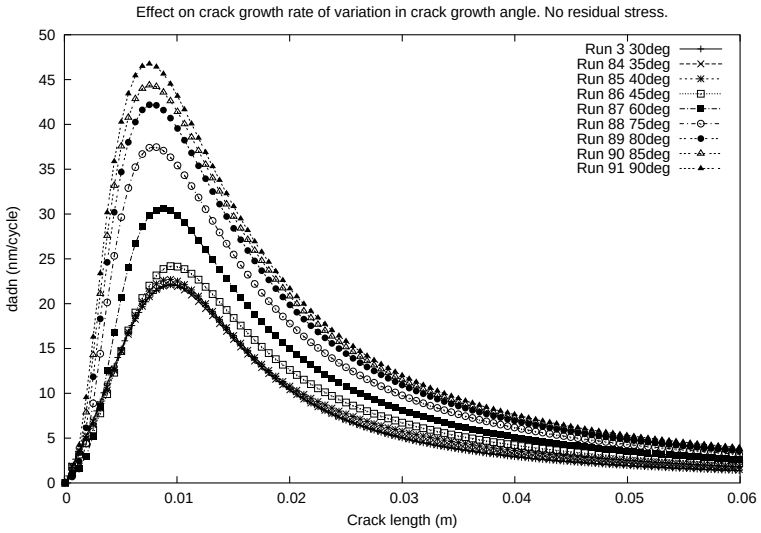

Figure 10: The effect of initial crack angle on crack growth rate. No residual stress present. Angles defined zero for a crack parallel to the rail surface, 90° for a crack normal to the surface. Maximum Hertzian contact pressure 1500MPa, surface and crack face friction coefficient 0.18.

Once cracks reach 60° or above, their growth rate becomes insensitive to the crack angle. The branching of cracks which initially lie at angles greater than 30° is still under investigation. Again, the trends found here may be specific to the residual stress input distribution used.

4.5 Effect of contact parameters on crack growth rates

4.5.1 Contact pressure

Both with and without residual stress present the variation of contact pressure produces dramatic variations in the predicted crack growth rate (Figure 12). Considering the peak growth rate predicted for cracks of up to 30mm, the increase of contact pressure from 750MPa to 1500MPa gives approximately a 60% increase in the growth rate in the presence of residual stress, and the increase from 1500MPa to 3000MPa produces around a 400% increase in peak crack growth rate. From Figure 12 is can be seen that the influence of residual stress is greatest at low contact pressures, for which the residual stresses are large in proportion to the contact stress. At 3000MPa the residual stress has little effect on the crack growth rate until the cracks become long.

4.5.2 Crack face friction

Variation in crack face friction while leaving rail surface traction constant simulates the presence of fluid or lubricants inside a crack (e.g water or oil), but not

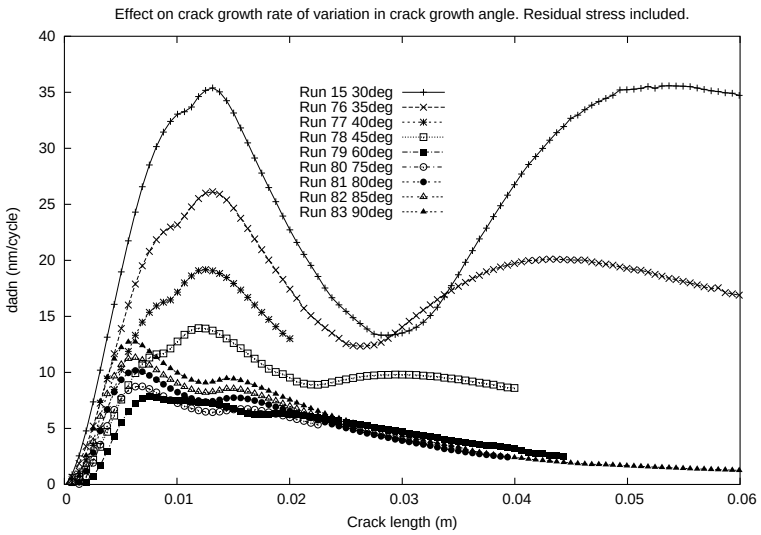

Figure 11: The effect of initial crack angle on crack growth rate. Residual stress applied with positive shear stress. Angles defined zero for a crack parallel to the rail surface, 90° for a crack normal to the surface. Maximum Hertzian contact pressure 1500MPa, surface and crack face friction coefficient 0.18.

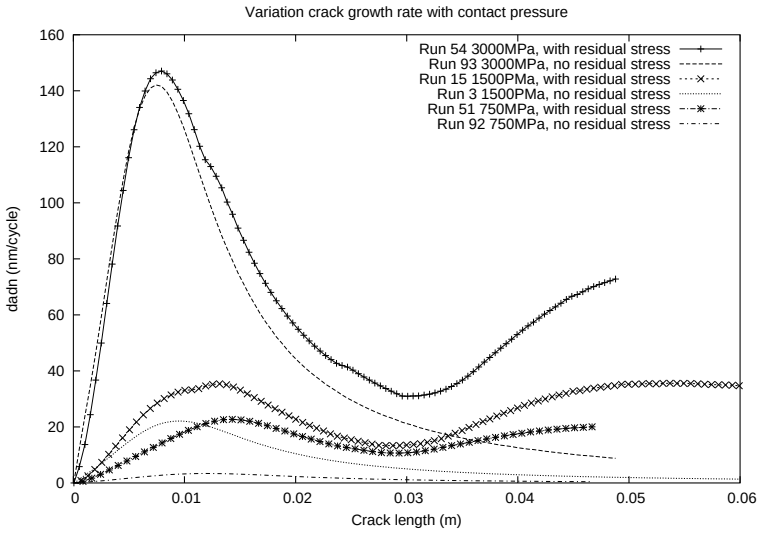

Figure 12: The effect of contact pressure on crack growth rate. Residual stress applied with positive shear stress, maximum Hertzian contact pressure 1500MPa, surface and crack face friction coefficient 0.18.

on the rail surface. This may occur when rain fills cracks with water, but the surface subsequently dries out, or when a flange lubricant is applied intermittently (faulty lubricator) causing lubricant to enter cracks and stay there, but also allowing its removed from the rail surface.

The results in Figure 13 show that both with and without residual stresses, shorter cracks (less than 30mm) are sensitive to these changes in crack face friction, but longer ones are much less so. As would be expected, the predicted crack growth rate rises with reduction in crack face friction level. This is because the crack faces are able to slide over one another more easily, and the shear forces driving their growth are less restricted when the friction between the faces is reduced. This is a similar effect to the application of tensile continuously welded rail stress (Section 4.3), although in that case the faces slide more easily because the normal force pressing them together is reduced. Without residual stress the changes in crack growth rate with crack face friction variation are similar to those with residual stress present, but the crack growth rates are lower.

4.5.3 Surface and crack face friction

Variation of surface and crack face friction levels together represents the case of similar conditions both on the rail surface and inside surface breaking cracks. Examples are completely dry conditions (high friction coefficients on the surface and inside the cracks), or grease based flange lubrication (low friction conditions on the surface and inside the cracks).

The results shown in Figure 14 indicate a similar trend to that shown in

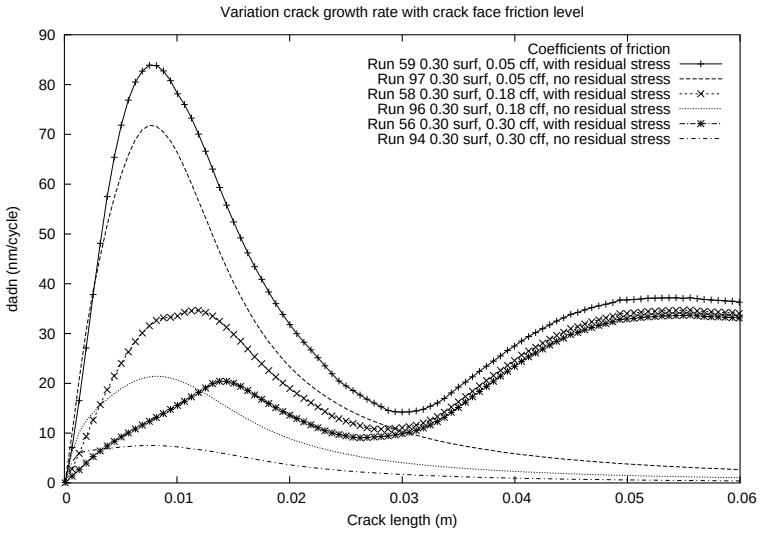

Figure 13: The effect of crack face friction coefficient on crack growth rate. Residual stress applied with positive shear stress, maximum Hertzian contact pressure 1500MPa, surface and crack face friction coefficient 0.18.

Figure 13 in that shorter cracks are much more sensitive to friction variation than are longer cracks. The combined effect of reducing both surface and crack face friction together is to increase crack growth rate. The reduction of these friction coefficients from 0.30 to 0.05 produces over a 500% increase in peak crack growth rate in the presence of residual stress. Patterns are similar for the cases with and without residual stress, but again, the crack growth rates without residual stress included in the model are lower.

5 Conclusions

The effect of longitudinal, vertical and shear residual stresses in rails on the growth rates and branching directions of inclined surface breaking cracks has been calculated. A range of residual stresses may act on a crack depending on its location in the rail head, and these stresses will also vary between rails depending on their manufacture, material properties, and loading history. Only a single set of residual stress data have been considered here, and the results are specific to those input data.

For the residual stress distribution considered, its inclusion in the modelling of a crack at 30° below the rail surface shows that the residual stresses increased the tendency of the crack to branch down into the rail, but this effect did not begin until the crack exceeded 20-25mm in length.

The sensitivity of crack growth rates to the magnitude of residual stresses was investigated by artificially raising and lowering the stress applied. This

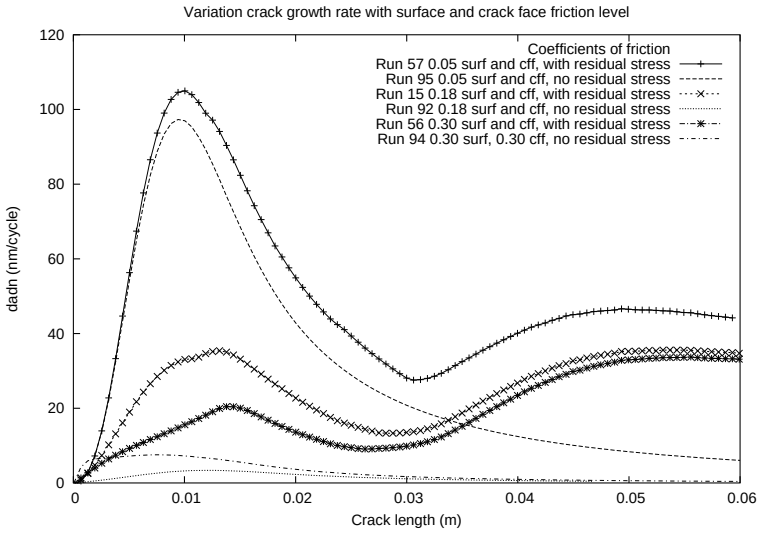

Figure 14: The effect of surface and crack face friction coefficient on crack growth rate. Residual stress applied with positive shear stress, maximum Hertzian contact pressure 1500MPa, surface and crack face friction coefficient 0.18.

indicated high sensitivity of growth rates to the magnitude of residual stresses, implying that using the correct distribution for the rail under study will be important in producing useful crack growth rate predictions.

The application of continuously welded rail (CWR) stress to the rail was modelled by taking the extreme case of temperature change of $\pm 40°$C either side of the rail neutral temperature. It was found that tensile CWR stress (cold rails) could produce around a 70% rise in crack growth rate over that of no CWR stress. Compressive residual stresses (hot rails) had almost no effect on crack growth rates. These differences were attributed to the degree to which cracks were pulled open or pushed closed by the longitudinal CWR stresses.

The sensitivity of crack growth rate to the initial crack angle (not branch angle) was investigated. It was found that the trend in the case without residual stress was for predicted crack growth rate to increase with increasing crack angle. With residual stresses present this trend was reversed, with 30° cracks showing the highest growth rates of those examined (30° is the smallest angle currently modelled), and the growth rate of cracks of 60° or above showing insensitivity to crack angle.

Trends in crack growth rate with variations in contact pressure, crack face friction and surface friction levels were investigated. These trends were largely similar for cases with and without residual stresses applied.

References

[1] A Kapoor and D I Fletcher. Post Hatfield rolling contact fatigue. The effect of residual stress on contact stress driven crack growth in rail. Part 1: The model. Technical Report WR061106-2, Newcastle University, November 2006.

[2] A Kapoor and D I Fletcher. Post Hatfield rolling contact fatigue. The effect of residual stress on contact stress driven crack growth in rail. Literature review. Technical Report WR061106-1, Newcastle University, November 2006.

[3] M Kaneta, H Yatsuzuka, and Y Murakami. Mechanism of crack growth in lubricated rolling/sliding contact. *ASLE Transactions*, 28(3):407–414, 1985.

[4] A Kapoor and D I Fletcher. Whole life rail model, stage 1 final report. Technical Report MEC/AK/AEAT/June01/, The University of Sheffield and AEAT, 2001.

[5] P E Bold, M W Brown, and R J Allan. Shear mode crack growth and rolling contact fatigue. *Wear*, 144:307–317, 1991.